Bismuth-induced increase of the magneto-optical effects in iron garnets: a theoretical analysis

2002 J. Phys.: Condens. Matter 14 6957

(http://iopscience.iop.org/0953-8984/14/28/307)

INSTITUTE OF PHYSICS PUBLISHING JOURNAL OF PHYSICS: CONDENSED MATTER

J. Phys.: Condens. Matter **14** (2002) 6957–6968 PII: S0953-8984(02)34400-X

Bismuth-induced increase of the magneto-optical effects in iron garnets: a theoretical analysis

A V Zenkov[1] **and A S Moskvin**

Department of Theoretical Physics, Ural State A M Gorky University, Lenin Ave., 51, 620083 Ekaterinburg, Russia

E-mail: andreas@r66.ru (A V Zenkov)

Received 28 February 2002
Published 5 July 2002
Online at stacks.iop.org/JPhysCM/14/6957

Abstract

In the framework of the concept of charge-transfer transitions, we suggest a semi-quantitative model which explains the strong increase of the circular magneto-optical effects in the iron garnets (IG) $R_3Fe_5O_{12}$ upon doping with Bi^{3+} or Pb^{2+} ions. The covalent admixture of Bi^{3+}, Pb^{2+} 6p orbitals (with giant one-electron spin–orbit coupling constant) with oxygen 2p states causes growth of the oxygen contribution to the spin–orbit coupling constant of $(FeO_6)^{9-}$, $(FeO_4)^{5-}$ complexes (the main magneto-optically active centres of IG). The enhanced spin–orbit interaction of the oxygen is not the only effect of substitution; it also gives rise to the effective anisotropic tensor addend to the spin–orbit interaction and the circular magneto-optical effects in IG as well. A computer simulation of the magneto-optical spectra of $Y_{3-x}Bi_xFe_5O_{12}$ for the case of an inhomogeneous bismuth distribution is carried out. Estimates of various contributions to the IG magneto-optical effects are given. The anisotropic tensor mechanism yields a contribution to the Faraday effect which is comparable in magnitude with the 'ordinary' ferromagnetic contribution.

Analysis of experimental data on the magneto-optical effects in garnets supports our theoretical model.

1. Introduction

The circular magneto-optical effects in the iron garnets (IG) $R_3Fe_5O_{12}$ is known to increase strongly even upon a relatively small admixture of isoelectronic Bi^{3+}, Pb^{2+} ions substituting for the rare-earth R ions in the IG lattice. This phenomenon has been dealt with in many papers (see for example [1–8]), but its *origin* is not yet clear. The problem is especially important since bismuth-substituted IG have found manifold applications in research and technology [9].

[1] Author to whom any correspondence should be addressed.

In most cases, the analysis is restricted to the (questionable) assignment of transitions in magneto-optical spectra (see [3–8]).

Among the rare papers where attempts at explanations have been made, note for example [1] where the following (qualitative) mechanisms for the lead-induced increase of the circular magneto-optical effects in IG are proposed:

(a) the intra-atomic orbital-promotion s^2–sp ($^1S_0$–$^3P_1$) transition in Pb^{2+} ions;

(b) photoinduced electron exchange between Fe^{3+} and Fe^{4+} ions (the latter arising as charge compensation of Pb^{2+} ions);

(c) the charge-transfer (CT) transition involving Pb^{2+} cation and anions.

The main shortcoming of these *ad hoc* hypotheses is their inapplicability as regards explaining the Bi-induced increase of the circular magneto-optical effects, which undoubtedly should have the same origin as the lead-induced one. The unsuitability of hypothesis (b) for the 'bismuth' case is immediately obvious. Mechanism (c), which is essentially related to the energy level structure of ions in the crystal, would yield different results for Bi- and Pb-substituted garnets, but the analysis of *differences* in effects obtained by subtracting the magneto-optical spectrum of pure IG from that of Bi-substituted IG and that of Pb-substituted IG shows in fact *identical* influences of these dopants on the spectral peculiarities of the circular magneto-optical effects in the near-ultraviolet range. This also argues against hypothesis (a), since the transition in the Bi^{3+} ion is situated too far ($\hbar\omega_0 \approx 4.3$ eV [10]) from the region $\hbar\omega_0 \approx 3$ eV of appreciable influence of Bi admixture[2] (in Pb^{2+} ions, the corresponding transition is considerably lower in energy).

A much more promising hypothesis is suggested, in particular, in [2] (on a merely qualitative level, though). Taking into account the giant values (17 000 and 14 500 cm^{-1} [2]) of the one-electron spin–orbit coupling constant ζ_{6p} for 6p orbitals of Bi^{3+} and Pb^{2+} ions[3], respectively, it relates the increase in the circular magneto-optical effects in Bi-substituted and Pb-substituted IG with the covalent admixture of Bi 6p and Pb 6p orbitals with the oxygen 2p orbital.

On the basis of this idea, we have built up the semi-quantitative model presented below. Analysis of experimental optical data and data on the circular magneto-optical effects in pure and Bi-substituted IG enabled us to obtain reasonable values of microscopic parameters for our theory—in contrast with the case for many papers [3–8], where in fact *the only* objective is the fitting of experimental spectra without any microscopic foundation for the results.

The paper is organized as follows. In section 2, we describe various contributions to the spin–orbit interaction which arise owing to the bismuth (lead) admixture in the IG. In section 3, we present the microscopic mechanisms of the magneto-optical effects in IG. In section 4, we briefly describe the technique that we use for theoretical processing of the optical and magneto-optical spectra of IG. We also report here the estimates of the microscopic parameters of our theory which result from the processing. In section 5, we obtain various contributions to the circular magneto-optical effects in IG and analyse them in a computer simulation. Finally, a summary is given in section 6.

This paper is a logical continuation of our earlier article [11].

[2] Thus, in the near-UV range $\hbar\omega_0 \approx 3$–4 eV, this transition contributes only to the *monotonic* intensity change of the magneto-optical spectral lines which are due to other mechanisms. The nearer the corresponding line is to the line of the actual Bi transition, the stronger this change would be. However, the monotonic change does not really take place.

[3] For brevity, we speak hereafter of the Bi inclusion only, but keeping in mind the Pb case as well.

2. Spin–orbit interaction in the presence of bismuth admixture

The effects of $2p(O^{2-})$–$6p(Bi^{3+})$ orbital overlap and the virtual transfer of a 2p electron from the O^{2-} ion to the empty bismuth 6p shell cause the wavefunction of the outer 2p electrons of the O^{2-} ion nearest to Bi^{3+} to acquire admixture of its 6p states:

$$\varphi_{2pm} \to \psi_{2pm} = \varphi_{2pm} - \sum_{m'} \langle 6pm'|2pm\rangle^* \varphi_{6pm'}, \tag{1}$$

where φ_{2p} and φ_{6p} are atomic wavefunctions. The integral $\langle 6pm'|2pm\rangle^* = \langle 2pm|6pm'\rangle$ of 2p–6p overlap can be written as

$$\langle 2pm|6pm'\rangle = \sum_{kq} (-1)^{1-m} \begin{pmatrix} 1 & k & 1 \\ -m & q & m' \end{pmatrix} \gamma_k C_q^k(\boldsymbol{R}), \tag{2}$$

where $\begin{pmatrix} \cdots \\ \cdots \end{pmatrix}$ is the Wigner $3j$-symbol [12], C_q^k is the spherical tensor of rank k (even values only; $k = 0$ and 2 (see below, section 5)), $C_q^k = \sqrt{4\pi/(2k+1)}Y_{kq}$, Y_{kq} being the spherical function; $\boldsymbol{R}$ is the unit vector in the O–Bi bond direction; γ_k is the covalency parameter; clearer are the linear combinations of γ_0, γ_2 corresponding to the covalency parameters for σ- and π-bonds:

$$\langle 6p_z|2p_z\rangle \equiv \langle 6p0|2p0\rangle \equiv \gamma_\sigma = \frac{1}{\sqrt{3}}\gamma_0 - \frac{2}{\sqrt{30}}\gamma_2,$$

$$\langle 6p_x|2p_x\rangle \equiv \langle 6p \pm 1|2p \pm 1\rangle \equiv \gamma_\pi = \frac{1}{\sqrt{3}}\gamma_0 + \frac{1}{\sqrt{30}}\gamma_2.$$

The bismuth 6p shell is characterized by very strong spin–orbit interaction:

$$V_{so} = \zeta_{6p} \sum_{\alpha=1}^{3} (-1)^\alpha \hat{l}_\alpha \hat{s}_{-\alpha} \tag{3}$$

(the scalar product of the orbital and spin angular momenta $\hat{l}$, $\hat{s}$ is written in spherical components [12]). Owing to the covalency effects, the virtual $2p \to 6p$ transition of an electron from oxygen to the bismuth 6p shell causes the increase of V_{so} on the oxygen ion. However, the role of Bi admixture is not restricted to this 'trivial' effect: the spin–orbit interaction itself is changing and becoming anisotropic and tensorial.

Considering the matrix element $\langle 2pm_1|V_{so}|2pm_2\rangle$ of the operator (3) on the hybrid wavefunctions ψ_{2pm} (1) results in the *effective* spin–orbit interaction on the oxygen ion:

$$V_{so}^{eff}(2p) = V_{so} + \Delta V_{so}^{iso} + \Delta V_{so}^{an}, \tag{4}$$

where the terms having the following meaning:

- V_{so}, given by
$$V_{so} = \zeta_{2p}(\boldsymbol{l} \cdot \boldsymbol{s}), \tag{5}$$
is the ordinary (existing even in the absence of bismuth substitution) spin–orbit interaction;
- ΔV_{so}^{iso} is the *isotropic* addend to V_{so} due to the Bi-induced increment $\Delta\zeta_{2p}$ of the effective one-electron spin–orbit coupling constant of the 2p shell:
$$\Delta V_{so}^{iso} = \Delta\zeta_{2p}(\boldsymbol{l} \cdot \boldsymbol{s}), \tag{6}$$
where
$$\Delta\zeta_{2p} = \tfrac{1}{3}\gamma_\pi(2\gamma_\sigma + \gamma_\pi)\zeta_{6p}. \tag{7}$$
At reasonable estimated values $|\gamma_\sigma| = |\gamma_\pi| \approx 0.4$ (see section 4), according to (7) we have $\Delta\zeta_{2p} \approx 4000\ cm^{-1}$ per Bi^{3+} ion. This value is larger by an order of magnitude than the one-electron spin–orbit coupling constant for iron ($\zeta_{3d} \approx 420\ cm^{-1}$ [13]) and permits the 'oxygen' contribution to V_{so} to compete with the 'iron' contribution (see section 3).

- ΔV_{so}^{an} is the *anisotropic* tensor addend to V_{so}; it can be presented in irreducible tensorial form as the convolution of the spherical tensor with the tensor product of the operators of the orbital and spin angular momenta:

$$\Delta V_{so}^{an} = \sqrt{\tfrac{2}{3}}\gamma_\pi(\gamma_\pi - \gamma_\sigma)(C^2(\boldsymbol{R}) \cdot [\boldsymbol{l} \times \boldsymbol{s}]^2)_0^0 \zeta_{6p}. \tag{8}$$

In Cartesian coordinates, ΔV_{so}^{an} takes the form

$$\Delta V_{so}^{an} = \lambda_{ij} l_i s_j,$$

where the effective tensor λ_{ij} of the spin–orbit interaction—the analogue of the constant λ in the ordinary formula $V_{so} = \lambda(\boldsymbol{l} \cdot \boldsymbol{s})$—is given by

$$\lambda_{ij} = \gamma_\pi(\gamma_\sigma - \gamma_\pi)\zeta_{6p}(R_i R_j - \tfrac{1}{3}\delta_{ij}).$$

3. Microscopic mechanisms of magneto-optical effects in iron garnets

From the foregoing, it appears that the action of Bi^{3+} ions on the circular magneto-optical effects in IG is essentially related to the oxygen 2p states in $(FeO_6)^{9-}$, $(FeO_4)^{5-}$ complexes—the main magneto-optically active centres of ferrites[4]. This strongly confirms the concept of ligand (O^{2-} ion)-to-iron CT transitions in these complexes (like ${}^6A_{1g}$–${}^6T_{1u}$ in $(FeO_6)^{9-}$ and ${}^6A_1$–${}^6T_2$ in $(FeO_4)^{5-}$) [14–16] as the main source of the optical and magneto-optical effects in IG, since it is this concept which naturally takes into account the significance of the ligand states in ferrite.

The CT state of the complex is characterized by the presence of two unfilled shells—predominantly 3d type and predominantly the ligand 2p shell—and accordingly the effective spin–orbit coupling constant λ of the complex contains, generally speaking, two contributions:

$$\lambda = \lambda(3d) + \lambda(2p) \tag{9}$$

(values of λ for various CT states of $(FeO_6)^{9-}$, $(FeO_4)^{5-}$ complexes are given in table 1; the computation technique is described in [15]).

The increment of the constant ζ_{2p} due to ΔV_{so}^{iso} (equations (6), (7)) results in an increasing oxygen contribution[5] $\lambda(2p)$ (9). Thereby, the so-called *ferromagnetic* contribution (the first two terms in the following formula) to the IG gyration vector $\boldsymbol{g}$ grows—it is proportional to the ferromagnetic vectors $\boldsymbol{m}_a$, $\boldsymbol{m}_d$ of the IG sublattices a and d, respectively, and originates in the orbital splitting and mixing [16] of the excited ${}^6T_{1u}({}^6T_2)$ states by V_{so}:

$$\boldsymbol{g} = A_a \boldsymbol{m}_a + A_d \boldsymbol{m}_d + C\boldsymbol{H} \tag{10}$$

(A_a, A_d, C are coefficients of proportionality).

The last term in (10)—the *field* contribution to the gyration vector that is proportional to the external magnetic field $\boldsymbol{H}$ and related to the orbital splitting and mixing of excited ${}^6T_{1u}({}^6T_2)$ CT states by the orbital part of the Zeeman interaction $V_Z = \mu_B g_L(\boldsymbol{L} \cdot \boldsymbol{H})$—is not influenced by the bismuth addition at all. However, the role of the oxygen states in forming the field contribution to $\boldsymbol{g}$ is important anyway (the effective orbital Landé factors $g_L(2p)$ and $g_L(3d)$ are comparable in magnitude—see table 1).

As to the ferromagnetic contribution to $\boldsymbol{g}$, the influence of Bi admixture may be particularly significant for the CT transitions whose final state spin–orbit coupling constant λ contains only the ligand contribution $\lambda(2p)$ (e.g., transitions 3 and 5 in the $(FeO_6)^{9-}$ complex—see table 1).

[4] Besides the mechanism considered, $3d(Fe^{3+})$–$6p(Bi^{3+})$ hybridization is also possible, but the oxygen ion serves here as the intermediate; the contribution of this mechanism is small: $\sim\gamma$.

[5] Note that the one-electron constant ζ_{2p} is not equivalent to the constant λ pertaining to the many-electron state of the complex.

Table 1. Characteristics of CT states and CT transitions in octahedral (No 1–6) and tetrahedral (No 7–13) complexes of iron garnets.

No	CT transition [15]	Effective orbital Landé factor[a] g_L [15]	Effective spin–orbit coupling constant λ [15]	Energy (eV)		Oscillator strength[b] $f(\times 10^{-3})$	Line width[b] Γ (eV)
				SP-X_α DV-computation [15]	Fitting of $Y_{3-x}Bi_xFe_5O_{12}$ spectra [2]		
1	$t_{2u} \rightarrow t_{2g}$	$-\frac{1}{2} - \frac{1}{4}$	$\frac{1}{10}\zeta_{3d} + \frac{1}{20}\zeta_{2p}$	3.1	2.78	1.5	0.2
2	$t_{1u}(\pi) \rightarrow t_{2g}$	$\frac{1}{2} - \frac{1}{4}$	$-\frac{1}{10}\zeta_{3d} + \frac{1}{20}\zeta_{2p}$	3.9	3.6	40	0.3
3	$t_{2u} \rightarrow e_g$	$0 + \frac{1}{4}$	$-\frac{1}{20}\zeta_{2p}$	4.4	4.3	60	0.3
4	$t_{1u}(\sigma) \rightarrow t_{2g}$	$\frac{1}{2} + 0$	$-\frac{1}{10}\zeta_{3d}$	5.1	4.8	50	0.3
5	$t_{1u}(\pi) \rightarrow e_g$	$0 - \frac{1}{4}$	$\frac{1}{20}\zeta_{2p}$	5.3	—[d]	—[d]	—[d]
6[c]	$t_{1u}(\sigma) \rightarrow e_g$	$0 + 0$	$0 + 0$	6.4	—[d]	—[d]	—[d]
7	$1t_1 \rightarrow 2e$	$0 + 0.30$	$-0.06\zeta_{2p}$	3.4	3.4	10	0.4
8	$6t_2 \rightarrow 2e$	$-0.01 + 0.05$	$0.002\zeta_{3d} - 0.01\zeta_{2p}$	4.3	4.6	40	0.3
9	$1t_1 \rightarrow 7t_2$	$0.42 - 0.41$	$-0.09\zeta_{3d} + 0.08\zeta_{2p}$	4.5	—[d]	—[d]	—[d]
10	$5t_2 \rightarrow 2e$	$-0.07 + 0.13$	$0.02\zeta_{3d} - 0.03\zeta_{2p}$	5.0	—[d]	—[d]	—[d]
11	$6t_2 \rightarrow 7t_2$	$-0.43 + 0.16$	$0.09\zeta_{3d} - 0.03\zeta_{2p}$	5.4	5.1	185	0.3
12	$1e \rightarrow 7t_2$	$-0.42 + 0.11$	$0.09\zeta_{3d} - 0.02\zeta_{2p}$	5.6	—[d]	—[d]	—[d]
13	$5t_2 \rightarrow 7t_2$	$-0.49 + 0.24$	$0.10\zeta_{3d} - 0.05\zeta_{2p}$	6.0	—[d]	—[d]	—[d]

[a] Orbital Landé factors are presented as the sum of the 3d-contribution (the first term) and the ligand 2p-contribution.
[b] Data for $Y_3Fe_5O_{12}$ are given.
[c] The nonzero contribution to the circular magnetooptics due to the CT state corresponding to this transition arises in the mixing mechanism only [16, 17].
[d] In the simulation of experimental spectra, this transition is ignored, since it is beyond the measurements range (No 5, 6, 12,13) or is lying too close to the transition already taken into account, their lines being fused (No 9, 10).

Since $\lambda(2p)$ is appreciably smaller than $\lambda(3d)$, the contribution of such transitions to the ferromagnetic part of $\boldsymbol{g}$ in the unsubstituted IG is negligible; the Bi substitution resolves such transitions. In contrast, the CT transitions with the final state λ formed only by the 3d subsystem of the molecular orbital of the complex (e.g., transition 4 in $(FeO_6)^{9-}$ complex) would not be strongly influenced by the Bi admixture.

The ferromagnetic contribution (10) to the IG gyration vector due to the CT transitions in octahedral and tetrahedral complexes (indices a, d, respectively), in the *splitting* mechanism [16], is given by

$$\boldsymbol{g}_{a,d} = 2 \sum_{j={}^6T_{1u},{}^6T_2} \frac{\pi e^2 L N_{a,d}}{\hbar m_e \omega_{0j}} \lambda^j \langle \boldsymbol{S} \rangle f_j \frac{\partial F_1(\omega, \omega_{0j}, \Gamma_j)}{\partial \omega_{0j}}. \tag{11}$$

We use this formula below, in sections 4 and 5. Here $L = ([n_0^2 + 2]/3)^2$ is the Lorentz–Lorenz local field correction factor, $N_{a,d}$ is the concentration of Fe^{3+} ions in the a and d positions ($N_a = 0.8 \times 10^{22}$ cm^{-3}; $N_d = \frac{3}{2}N_a$ for the yttrium IG); λ^j is the spin–orbit coupling constant in the jth excited CT state; f_j is the oscillator strength for the jth CT transition; $\langle \boldsymbol{S} \rangle$ is the average spin. The Lorentzian dispersion factor F_1 has the form

$$F_1(\omega, \omega_0, \Gamma) = \frac{2(\omega + i\Gamma)}{(\omega + i\Gamma)^2 - \omega_0^2},$$

where ω_0 is the transition frequency, Γ is the linewidth.

Note that in the mechanism of *mixing* [16] the excited CT states, the formula for $\boldsymbol{g}$ which is analogous to (11) includes the dispersion factor F_1 causing the so-called 'paramagnetic' line shape, whereas the dispersion factor $\partial F_1/\partial\omega_0$ determines the 'diamagnetic' one. The

contributions of the splitting and mixing mechanisms are comparable in magnitude [14] and usually appear *simultaneously*.

Thereby we consider it rather trivial when an author begins reasoning regarding how many 'paramagnetic' and 'diamagnetic' transitions were *introduced* to obtain the 'best' (or 'excellent') fit to experimental data [3–6, 8]. The outwardly good agreement is not surprising when one bears in mind the multitude of 'degrees of freedom' (resonance frequencies, linewidths, etc). Without a *microscopic theoretical* basis, this agreement is unconvincing.

The field contribution to $\boldsymbol{g}$ (10) in the splitting mechanism is given by

$$\boldsymbol{g}_{\mathrm{a,d}} = 2 \sum_{j={}^6\mathrm{T}_{1u},{}^6\mathrm{T}_2} \frac{\pi e^2 L N_{\mathrm{a,d}}}{\hbar m_{\mathrm{e}} \omega_{0j}} \mu_{\mathrm{B}} g_{\mathrm{L}}^j \boldsymbol{H} f_j \frac{\partial F_1(\omega, \omega_{0j}, \Gamma_j)}{\partial \omega_{0j}}, \tag{12}$$

g_{L}^j being the effective orbital Landé factor for the jth CT state.

Note the possibility of an influence of bismuth upon the *quadratic* (in magnetization) magneto-optical effects in IG. To the second order of perturbation theory, the contribution to the polarizability tensor of the $(\mathrm{FeO}_6)^{9-}$ complex owing to the orbital splitting of excited ${}^6\mathrm{T}_{1u}$ states by the spin–orbit interaction is given by [17]

$$\alpha_{kl} = \frac{1}{2\sqrt{3}} \sum_{j={}^6\mathrm{T}_{1u}} \frac{e^2 (\lambda^j)^2 f_j}{\hbar^2 m_{\mathrm{e}} \omega_{0j}} \left\langle S_k S_l - \frac{1}{3} S(S+1) \right\rangle \frac{\partial^2 F_2(\omega, \omega_{0j}, \Gamma_j)}{\partial \omega_{0j}^2}, \tag{13}$$

where the Lorentzian dispersion function (different from F_1 above!) is

$$F_2(\omega, \omega_0, \Gamma) = \frac{2\omega_0}{(\omega + \mathrm{i}\Gamma)^2 - \omega_0^2}.$$

Thus, the Bi-induced increase of the spin–orbit coupling constant λ^j of the complex causing the growth of the *circular* magneto-optical effects should strengthen the *magnetic linear birefringence* as well. This effect should be even sharper, since the constant λ^j is here squared—in contrast with the case in (11).

Note also that the magnetic linear birefringence may be caused not only by V_{so}, but by the low-symmetry crystal field as well; the latter gives rise to the anisotropic *elasto-optical* contribution to α_{kl} [17] which does not depend on the Bi addition. However, the strong crystal lattice distortion by bismuth attests to the low symmetry of the crystal field parameters, and so this contribution also depends on the Bi concentration; but this dependence is not as simple as in (13).

4. Theoretical analysis of experimental spectra

We state here the technique used for theoretical processing of the optical and magneto-optical spectra of IG in this work.

To apply the formulae (11)–(13) one has to know the oscillator strengths f_j of the CT transitions. To this end we carried out a visual fitting of the spectral dependence of $\mathrm{Im}\,\alpha_0^0$—the imaginary part of the diagonal component of the irreducible polarizability tensor which determines the isotropic absorption in the garnet $\mathrm{Y_3Fe_5O_{12}}$. We used the data on the real and imaginary parts of the permittivity $\varepsilon_0 = \varepsilon_0' + \mathrm{i}\varepsilon_0''$ from [2]. In cubic dielectrics, α_0^0 and ε_0 obey the Clausius–Mossotti relation

$$\frac{\varepsilon_0 - 1}{\varepsilon_0 + 2} = \frac{4\pi}{3} N \alpha_0^0,$$

whence

$$\frac{4\pi}{3} N\, \mathrm{Im}\,\alpha_0^0 = \frac{3\varepsilon_0''}{(\varepsilon_0' + 2)^2 + (\varepsilon_0'')^2}. \tag{14}$$

For $\operatorname{Im}\alpha_0^0$ we have the formula [17]

$$\operatorname{Im}\alpha_0^0 = -\sum_j \frac{e^2\hbar f_j}{2m_e\omega_{0j}} \operatorname{Im} F_2(\omega, \omega_{0j}, \Gamma_j), \tag{15}$$

that we used for processing the fitting results.

In this way we have obtained the values (see table 1) of f_j, as well as ω_{0j} and Γ_j (the latter were estimated mainly from the fitting of the non-diagonal part ε^1 of the permittivity, but in compliance with (14), since the spectrum (14) itself is almost structureless).

In the framework of the CT transitions concept, with the values of the parameters ω_{0j}, Γ_j, f_j, etc (see table 1) characteristic of the yttrium IG, using the fitting procedures of the computations system MATHEMATICA, we have performed model processing of the experimental [2] spectra of the gyration vector z-component, $g_z(\omega)$, in the Bi-substituted garnets $Y_{3-x}Bi_xFe_5O_{12}$ ($x = 0.25, 0.8, 1.0$). We have taken into account both the allowed and a number of forbidden CT transitions in octahedral and tetrahedral complexes, considering the contributions of the mechanism of splitting of the states (with the dispersion dependence $\propto\frac{\partial F_1}{\partial\omega_0}$), as well as those due to the state mixing ($\propto F_1$). Figure 1 shows the model fitting $\operatorname{Re} g_z(\omega)$ spectral dependence and the result of the $\operatorname{Im} g_z(\omega)$ computation for $Y_{2.2}Bi_{0.8}Fe_5O_{12}$ with the same parameters (thin lines) as well as the experimental data [2] (thick lines)[6]. Generally, the model computation is in quite good agreement with experiment over a wide spectral range, 2–5 eV, which is strong evidence in favour of the concept of CT transitions being the main source of the circular magneto-optical effects in IG. We do not claim that our fit is absolutely reliable—especially in the high-energy region where plenty of 'octahedral' and 'tetrahedral' CT transitions are superimposed.

The processing results enabled us to estimate the value of $\Delta\zeta_{2p}$ at various Bi concentrations x in the garnet $Y_{3-x}Bi_xFe_5O_{12}$. Note that the model 'macroscopic observable' quantity $\Delta\zeta_{2p}^{\mathrm{mod}}$, depending on the concentration and lattice distribution of Bi ions, differs from the 'microscopic' quantity $\Delta\zeta_{2p}$ (7).

Assuming a *homogeneous* bismuth distribution over the crystal and equal probability (defined by the relative concentration $\xi = \frac{x}{3}$) for the Bi ion to occupy each of two c positions nearest to a given O^{2-} ion, we have

$$\Delta\zeta_{2p}^{\mathrm{mod}} = \Delta\zeta_{2p}[P_2(1) + 2P_2(2)],$$

where $P_n(k)$ is the probability of occupying k positions among the n that exist. Applying the binomial distribution formula $P_n(k) = C_n^k\xi^k(1-\xi)^{n-k}$ (C_n^k is the number of combinations) and taking into account eight Bi^{3+}–O^{2-} bonds for each Bi ion, we finally get

$$\Delta\zeta_{2p}^{\mathrm{mod}}(x) = \tfrac{16}{3}x\,\Delta\zeta_{2p}. \tag{16}$$

Thus, in the simplest model, neglecting the site preferences of Bi^{3+} ions in the crystal lattice, the changes of $\Delta\zeta_{2p}^{\mathrm{mod}}$ and the IG circular magneto-optical effects are both *linear* in the bismuth-ion concentration.

Using (7), (11), (16), as well as the data from table 1, one can evaluate the covalency parameters $\gamma_\sigma, \gamma_\pi$. For example, for the 'tetrahedral' CT transition with the lowest energy $\hbar\omega_0 = 3.4$ eV at $x = 0.25$, from (11) we obtain the model fitting value of the spin–orbit coupling constant $\lambda^{\mathrm{mod}} = -380\ \mathrm{cm}^{-1} = -0.06\,\Delta\zeta_{2p}^{\mathrm{mod}}$ (see table 1), whence, according to (16), $\Delta\zeta_{2p} \approx 4700\ \mathrm{cm}^{-1}$. In the rough approximation of covalency parameter equality $|\gamma_\sigma| = |\gamma_\pi| \equiv \gamma$, one can estimate these parameters using (7). For various Bi concentrations we obtain the following reasonable values:

[6] The same fitting quality for $\operatorname{Re}\boldsymbol{g}, \operatorname{Im}\boldsymbol{g}$ spectra cannot be achieved since the dependences $\operatorname{Re} g(\omega), \operatorname{Im} g(\omega)$ themselves result from *processing* of the experimental data in the framework of an *approximative* numerical algorithm.

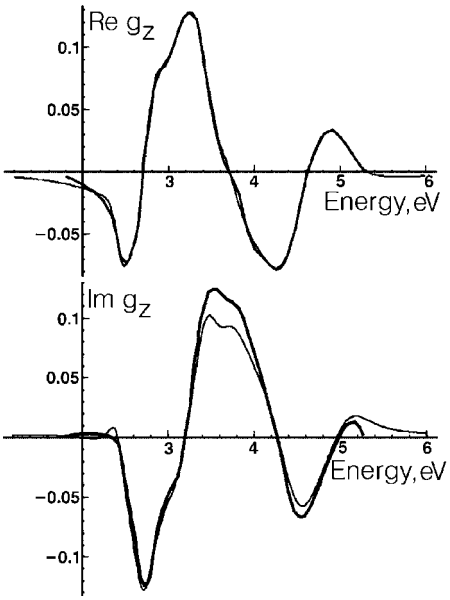

Figure 1. The z-component of the gyration vector of garnet $Y_{2.2}Bi_{0.8}Fe_5O_{12}$: the spectral dependences of the real and imaginary parts according to experimental data [2] (thick curves) and our model simulation (thin curves).

x	0.25	0.8	1.0
γ	0.53	0.47	0.42

Note the decrease of γ with growing Bi addition to IG—possibly owing to Bi-induced lattice distortion and the resulting change of the Bi–O bond geometry. Taking into account these distortions, as well as the eventual inhomogeneity of the Bi bulk distribution, would give rise to deviations from the linear concentration dependence of the circular magneto-optical effects in IG.

5. The tensor contributions to the IG magneto-optical effects

According to the Kramers–Heisenberg formula in the irreducible tensor form [16], the contribution to the components α^1_p of the antisymmetric part of $\hat{\alpha}$—the $(FeO_6)^{9-}$ complex polarizability tensor—owing to the allowed electric dipole CT transitions of $^6A_{1g}$–$^6T_{1u}$ (^6S–^6P) type is given by

$$\alpha^1_p = \frac{1}{\hbar}\sum_{j=^6T_{1u}}\sum_{r_1,r_2}\sum_{m_1,m_2}\begin{bmatrix}1 & 1 & 1\\ r_1 & r_2 & p\end{bmatrix} \times \langle 00|d_{r_1}|1m_1\rangle\langle 1m_1|V_{so}|1m_2\rangle\langle 1m_2|d_{r_2}|00\rangle\frac{\partial F_1(\omega,\omega_{0j},\Gamma_j)}{\partial\omega_0}$$

$$= \frac{1}{\hbar}\sum_{j=^6T_{1u}}\sum_{r_1,r_2}\sum_{m_1,m_2}(-1)^{-p}\sqrt{3}\begin{pmatrix}1 & 1 & 1\\ r_1 & r_2 & -p\end{pmatrix}(-1)^{1-m_1}\frac{1}{\sqrt{3}}\delta_{r_1,-m_1}$$

$$\times \langle 1m_1|V_{\rm so}|1m_2\rangle(-1)^{1-m_2}(-1)^{1-r_2}\frac{1}{\sqrt{3}}\delta_{r_2,m_2}|\langle 0\|d\|1\rangle|^2\frac{\partial F_1(\omega,\omega_{0j},\Gamma_j)}{\partial\omega_0}$$

$$= \frac{1}{\hbar\sqrt{3}}\sum_{j={}^6{\rm T}_{1u}}\sum_{m_1,m_2}(-1)^{-p-m_1-m_2+1-m_2}\begin{pmatrix}1 & 1 & 1\\ -m_1 & m_2 & -p\end{pmatrix}\langle 1m_1|V_{\rm so}|1m_2\rangle$$

$$\times |\langle 0\|d\|1\rangle|^2\frac{\partial F_1(\omega,\omega_{0j},\Gamma_j)}{\partial\omega_0}, \tag{17}$$

where $\begin{bmatrix}\cdots\\ \cdots\end{bmatrix}$ is the Clebsch–Gordan coefficient, d_r is the component of electric dipole moment. The matrix element $\langle 1m_1|V_{\rm so}|1m_2\rangle$ of the spin–orbit interaction contains the term (cf (2))

$$\left\langle \sum_{\substack{k_1,q_1\\ m_1'}}(-1)^{1-m_1}\begin{pmatrix}1 & k_1 & 1\\ -m_1 & q_1 & m_1'\end{pmatrix}\gamma_{k_1}C^{k_1}_{q_1}(\boldsymbol{R})\varphi_{6{\rm p}m_1'}\middle|\zeta_{6{\rm p}}\sum_\alpha(-1)^\alpha l_\alpha s_{-\alpha}\middle|\sum_{\substack{k_2,q_2\\ m_2'}}(-1)^{1-m_2}\right.$$

$$\left.\times\begin{pmatrix}1 & k_2 & 1\\ -m_2 & q_2 & m_2'\end{pmatrix}\gamma_{k_2}C^{k_2}_{q_2}(\boldsymbol{R})\varphi_{6{\rm p}m_2'}\right\rangle, \tag{18}$$

which can be rewritten by the Wigner–Eckart theorem as

$$\sum_{\substack{k_1,k_2\\ q_1,q_2}}\sum_{\substack{m_1',m_2'\\ \alpha}}(-1)^{-m_1-m_2+\alpha}\begin{pmatrix}1 & k_1 & 1\\ -m_1 & q_1 & m_1'\end{pmatrix}\begin{pmatrix}1 & k_2 & 1\\ -m_2 & q_2 & m_2'\end{pmatrix}$$

$$\times\gamma_{k_1}\gamma_{k_2}(-1)^{q_1}C^{k_1}_{-q_1}(\boldsymbol{R})C^{k_2}_{q_2}(\boldsymbol{R})(-1)^{1-m_1'}\begin{pmatrix}1 & 1 & 1\\ -m_1' & \alpha & m_2'\end{pmatrix}\sqrt{6}s_{-\alpha}\zeta_{6{\rm p}}, \tag{19}$$

where the product $C^{k_1}_{-q_1}(\boldsymbol{R})C^{k_2}_{q_2}(\boldsymbol{R})$ of spherical functions takes the form [12]

$$\sum_{kq}(2k+1)\begin{pmatrix}k_1 & k_2 & k\\ -q_1 & q_2 & q\end{pmatrix}\begin{pmatrix}k_1 & k_2 & k\\ 0 & 0 & 0\end{pmatrix}C^{k*}_q(\boldsymbol{R}). \tag{20}$$

By formulae (18)–(20), for α^1_p we have

$$\alpha^1_p = \frac{\sqrt{2}}{\hbar}\sum_{\substack{k_1,k_2\\ k,q\\ \alpha}}(-1)^{-p+k+k_1+1}(2k+1)\gamma_{k_1}\gamma_{k_2}C^k_{-q}(\boldsymbol{R})s_{-\alpha}|\langle 0\|d\|1\rangle|^2$$

$$\times\begin{pmatrix}k_1 & k_2 & k\\ 0 & 0 & 0\end{pmatrix}\frac{\partial F_1}{\partial\omega_0}\zeta_{6{\rm p}}\sum_{m_1,m_2}\sum_{q_1,q_2}\sum_{m_1',m_2'}(-1)^{k_1+k_2+q_2-q_1+m_1-m_2+m_2'-m_1'}$$

$$\times\begin{pmatrix}k_2 & k & k_1\\ -q_2 & -q & q_1\end{pmatrix}\begin{pmatrix}k_1 & 1 & 1\\ -q_1 & -m_1' & m_1\end{pmatrix}\begin{pmatrix}1 & 1 & 1\\ -m_1 & -p & m_2\end{pmatrix}$$

$$\times\begin{pmatrix}1 & k_2 & 1\\ -m_2 & q_2 & m_2'\end{pmatrix}\begin{pmatrix}1 & 1 & 1\\ -m_2' & -\alpha & m_1'\end{pmatrix} \tag{21}$$

(for brevity, we show here and in the following the contribution of one CT transition only).

In the triple sum, there arises a standard sum over momenta projections [12] which yields the final expression:

$$\alpha^1_p = \frac{\sqrt{2}}{\hbar}\sum_{\substack{k_1,k_2\\ k,q\\ \alpha}}(-1)^{-p+k+k_1}(2k+1)\gamma_{k_1}\gamma_{k_2}C^k_{-q}(\boldsymbol{R})s_{-\alpha}$$

$$\times|\langle 0\|d\|1\rangle|^2\begin{pmatrix}k_1 & k_2 & k\\ 0 & 0 & 0\end{pmatrix}\frac{\partial F_1}{\partial\omega_0}\zeta_{6{\rm p}}\begin{pmatrix}k & 1 & 1\\ q & p & \alpha\end{pmatrix}\begin{Bmatrix}k & 1 & 1\\ k_2 & 1 & 1\\ k_1 & 1 & 1\end{Bmatrix}, \tag{22}$$

where $\langle 0\|d\|1\rangle$ is the reduced matrix element of the electric dipole moment $\boldsymbol{d}$, $\left\{\begin{smallmatrix}\cdot&\cdot&\cdot\\ \cdot&\cdot&\cdot\end{smallmatrix}\right\}$ is the $9j$-symbol [12].

Note that formula (8) ensues from another form of momenta coupling.

By physical reasons, the index k must be even, since otherwise the space inversion $\boldsymbol{R}\to-\boldsymbol{R}$ would change the sign of $C^k(\boldsymbol{R})$ and that of the whole expression (22) as well. The triangle rule for $9j$-symbols and the requirement of an even sum of the upper-row elements in

$$\begin{pmatrix} k_1 & k_2 & k\\ 0 & 0 & 0\end{pmatrix}$$

admit then values $k=0$ and 2 only. The value $k=0$ corresponds to the *isotropic scalar* coupling of the antisymmetric part of the polarizability tensor $\hat{\alpha}$ and the average spin $\langle\hat{\boldsymbol{s}}\rangle$ (cf with (6)); the *anisotropic tensorial* contribution to α^1 (cf (8)) arises at $k=2$.

The following formulae represent: the *isotropic* contribution

$$\begin{aligned}\boldsymbol{\alpha} &= \frac{\sqrt{2}}{\hbar}\left[-\frac{1}{9}\gamma_0^2+\frac{1}{90}\gamma_2^2\right]|\langle 0\|d\|1\rangle|^2\frac{\partial F_1}{\partial\omega_0}\zeta_{6\mathrm{p}}\langle\boldsymbol{s}\rangle\\ &= -\frac{\sqrt{2}}{9\hbar}\gamma_\pi(\gamma_\pi+2\gamma_\sigma)|\langle 0\|d\|1\rangle|^2\frac{\partial F_1}{\partial\omega_0}\zeta_{6\mathrm{p}}\langle\boldsymbol{s}\rangle;\end{aligned}\tag{23}$$

the *anisotropic* contribution in the irreducible tensor form

$$\begin{aligned}\alpha^1_p = {}&\frac{5\sqrt{2}}{\hbar}\frac{\partial F_1}{\partial\omega_0}\zeta_{6\mathrm{p}}|\langle 0\|d\|1\rangle|^2\sum_{k_1,k_2=0,1,2}\sum_{q=-2}^{2}\sum_{\alpha=-1}^{1}(-1)^{-p+k_1}\\ &\times\begin{pmatrix}2&1&1\\ q&p&\alpha\end{pmatrix}\begin{Bmatrix}2&1&1\\ k_2&1&1\\ k_1&1&1\end{Bmatrix}\gamma_{k_1}\gamma_{k_2}C^{\,2}_{-q}(\boldsymbol{R})s_{-\alpha}\begin{pmatrix}k_1&k_2&2\\ 0&0&0\end{pmatrix};\end{aligned}\tag{24}$$

and the same, but in the Cartesian form,

$$\boldsymbol{\alpha}=\frac{\sqrt{2}}{6\hbar}\gamma_\pi(\gamma_\sigma-\gamma_\pi)|\langle 0\|d\|1\rangle|^2\frac{\partial F_1}{\partial\omega_0}\zeta_{6\mathrm{p}}\hat{\Lambda}\langle\boldsymbol{s}\rangle.\tag{25}$$

The tensor $\hat{\Lambda}$ is given by

$$\begin{pmatrix}\sin^2\theta\cos2\varphi-\frac{1}{3}(3\cos^2\theta-1) & \sin^2\theta\sin2\varphi & \sin2\theta\cos\varphi\\ \sin^2\theta\sin2\varphi & -\sin^2\theta\cos2\varphi-\frac{1}{3}(3\cos^2\theta-1) & \sin2\theta\sin\varphi\\ \sin2\theta\cos\varphi & \sin2\theta\sin\varphi & \frac{2}{3}(3\cos^2\theta-1)\end{pmatrix}$$

where θ and φ are polar angles of $\boldsymbol{R}$—the unit vector in the O^{2-}–Bi^{3+} bond direction.

Using (25), we have computed the gyration vector $\boldsymbol{g}=4\pi NL\boldsymbol{\alpha}$ and the specific Faraday rotation $\theta_\mathrm{F}=\frac{\omega}{2n_0c}\,\mathrm{Re}(\boldsymbol{g}\cdot\boldsymbol{n})$, where $\boldsymbol{n}$ is the unit vector in the light propagation direction, n_0 is average refraction index for two circularly polarized waves. The computation was carried out for the cubiform cluster consisting of eight unit cells of IG with atom positions from [18] and cell parameters of $Y_3Fe_5O_{12}$ [19] (both atom positions and cell parameters have been assumed independent of Bi concentration).

The nearest oxygen ions have been found for each c position and corresponding contributions to $\boldsymbol{\alpha}$ (25) summed. We considered several variants of Bi^{3+}-ion substitution into c positions:

(1) All c positions of the IG unit cell are occupied with Bi ions.
(2) Only positions 1–3 and 10–12 (and those reached by translations $\{\frac{1}{2},\frac{1}{2},\frac{1}{2}\}$) are occupied; the position numbering here and below is according to [18].
(3) Only positions 4–9 (and those reached by translations $\{\frac{1}{2},\frac{1}{2},\frac{1}{2}\}$) are occupied.

Cases (2) and (3) correspond to (111)-oriented IG film where two coextensive sets of crystallographically non-equivalent positions arise.

The computation has shown that the contribution to α due to Bi^{3+} ions occupying positions 4–9 and their equivalents is about eight times the contribution of Bi ions in positions 1–3 and 10–12 and their equivalents (of course, the sum of the two contributions is the same as in case (1)).

At the wavelength 0.6 μm, the specific Faraday rotation θ_F corresponding to the computed data and the parameters characteristic of the CT transitions in IG reaches a magnitude of about 6×10^3 deg cm^{-1} for the contribution of the 'anisotropic' mechanism. The 'isotropic' mechanism (23) yields $\theta_F \approx 3 \times 10^5$ deg cm^{-1} which is larger by more than an order of magnitude than the contribution of the 'ordinary' spin–orbit interaction (11).

6. Conclusions

To conclude, we point out an essential feature of the approach adopted in this work. It consists in neglecting the electronic–vibrational character of CT states and transitions, when one takes into account the *electronic* component of the wavefunction only. The exactness of the model computation achieved does not exclude the presence of a small (about 10%) so-called *vibronic* reduction of matrix elements of orbital operators. The reduction is caused by electronic–vibrational interactions and manifests itself in a possible (potentially very large) decrease of the absolute value of the purely electronic g_L, λ parameters. The vibronic reduction of the Bi-induced contribution to the spin–orbit coupling constant of CT states may differ from that of the Fe 3d contribution. A thorough analysis of electronic–vibrational interactions in CT states is rather difficult, owing to the existence of two unfilled shells in the electronic configurations of CT states—predominantly ligand 2p and Fe 3d shells.

The following inferences may be drawn from the analysis presented:

(1) The Bi^{3+} ions induce, owing to the contribution of ligand orbitals in $(FeO_6)^{9-}$, $(FeO_4)^{5-}$ complexes, an effective anisotropic spin–orbit interaction in CT states. The parameters of this interaction depend on the geometry of the Fe^{3+}–O^{2-}–Bi^{3+} bond, the type of the CT state, and the type of the complex (octahedron, tetrahedron).
(2) Bi-induced contributions to the circular magneto-optical effects are particularly appreciable when the 3d contribution is absent (for example, in Cu^{2+}-based complexes).
(3) Bi substitution would hardly influence the field contribution to the circular magneto-optical effects in IG.
(4) Bi substitution strongly augments the anisotropic magnetic birefringence of 'spin–orbit' origin.
(5) The model fitting of experimental spectral dependences of the circular magneto-optical effects in Bi-containing IG enabled us to obtain physically reasonable estimates of parameters for the suggested theoretical model.
(6) In the framework of the model suggested, theoretical estimates of Bi-induced contributions to the IG magneto-optical effects are obtained. The anisotropic tensor mechanism yields a contribution to the Faraday effect which is comparable in magnitude with the 'ordinary' ferromagnetic contribution.

Acknowledgment

This work was financially supported by grant No REC-005 of CRDF.

References

[1] Scott G B, Lacklison D E and Page J L 1974 *Phys. Rev.* B **10** 971
[2] Wittekoek S, Popma T J A, Robertson J M and Bongers P F 1975 *Phys. Rev.* B **12** 2777
[3] Šimša Z, Šimšova J, Zemanova D, Čermak J and Nevriva M 1984 *Czech. J. Phys.* B **34** 1102
[4] Dionne G F and Allen G A 1993 *J. Appl. Phys.* **73** 6127
[5] Allen G A and Dionne G F 1993 *J. Appl. Phys.* **73** 6130
[6] Dionne G F and Allen G A 1994 *J. Appl. Phys.* **75** 6372
[7] Shinagawa K 1999 *Magnetooptics* ed S Sugano and N Kojima (Berlin: Springer) pp 137–77
[8] Helseth L E, Hansen R W, Il'yashenko E I, Baziljevich M and Johansen T H 2001 *Phys. Rev.* B **64** 174406
[9] Zvezdin A K and Kotov V A 1997 *Modern Magnetooptics and Magnetooptical Materials* (Bristol: Institute of Physics Publishing)
[10] Wittekoek S and Lacklison D E 1972 *Phys. Rev. Lett.* **28** 740
[11] Moskvin A S and Zenkov A V 1991 *Solid State Commun.* **80** 739
[12] Varshalovich D A, Moskalev A N and Khersonskii V K 1988 *Quantum Theory of Angular Momentum* (Singapore: World Scientific)
[13] Krebs J J and Maisch W G 1971 *Phys. Rev.* B **4** 757
[14] Zenkov A V and Moskvin A S 1990 *Fiz. Tverd. Tela* **32** 3674 (in Russian)
[15] Moskvin A S, Zenkov A V, Yuryeva E I and Gubanov V A 1991 *Physica* B **168** 187
[16] Ganshina E A, Zenkov A V, Koptsik S V, Krinchik G S, Moskvin A S and Trifonov A Yu 1990 Charge-transfer transitions and magneto-optics of ferrites *VINITI, USSR, Paper No788-B90* (in Russian)
[17] Zenkov A V 1990 Origin of magneto-optic properties of ferrites *PhD Thesis* Ural State University, Sverdlovsk
[18] *International Tables for X-Ray Crystallography* 1952 vol 1 (Birmingham: Kynoch)
[19] Geller S 1967 *Z. Kristallogr.* **125** 1